Proceedings of Global Power and Propulsion Society
ISSN-Nr: 2504-4400
GPPS Hong Kong 2023
October 17-19, 2023
www.gpps.global

GPPS-TC-2023-0050

THE ESTABLISHMENT OF CASCADE EXPERIMENTAL SAMPLE BANK AND THE MODIFICATION OF EMPIRICAL MODEL

Xiaolong Xing
School of Power and Energy, Northwestern Polytechnical University
Email:toughmirror@gmail.com
Xi'an,Shaanxi,China

Qidong Chen
School of Power and Energy, Northwestern Polytechnical University
Email:cqd@mail.nwpu.edu.cn
Xi'an,Shaanxi,China

Bo Liu
School of Power and Energy, Northwestern Polytechnical University
Email:liubo704@nwpu.edu.cn
Xi'an,Shaanxi,China

ABSTRACT

Based on 1548 test conditions obtained from 24 groups of axial compressor cascade test, a cascade aerodynamic performance sample library is established. On this basis, a typical reference deviation angle model and a off-design deviation angle model are selected respectively. Then, aiming at the problem of poor accuracy of traditional empirical model in high load cascade performance prediction, the key coefficients in the model were optimized by genetic optimization method based on the established cascade performance sample library, and the calculation error of the optimized deviation angle model was reduced by 39.9%. Finally, the accuracy and universality of the improved model are verified by calculating and predicting the aerodynamic performance of a multistage compressor.

INTRODUCTION

In the process of two-dimensional design of compressor, two-dimensional flow calculation (Xu, J, 2017; Wu C, 1952) is the main method of calculation. Based on S1, S2 flow surface theory and a series of reasonable assumptions, the flow problem of compressor on the meridional flow surface can be transformed into a problem of solving one-dimensional ordinary differential equation. Combined with the calculation idea of streamline curvature method (Wu, X et al., 2017; Novak R A, 1967), the flow field parameters can be quickly estimated on the meridional plane of compressor. The main equation of the streamline curvature method is derived based on the inviscid assumption, in order to account for the influence of viscosity on the fluid, performance models, such as deviation angle models, need to be introduced. To a certain extent, the accuracy of the prediction results of the streamline curvature method depends on the rationality of the deviation angle models. In the early stage, many compressor deviation angle models were established and modified based on the experimental data of many linear cascades. Because the flow condition in linear cascades is different from the three-dimensional flow condition of the real compressor, the applicability of the model and the accuracy of the model prediction have many limitations, and the induced deviation will be more obvious in the prediction of off-design conditions. Domestic and foreign scholars have been trying to improve the accuracy of performance models, they have put forward a large number of different performance models, but the performance models have a certain range of application, once beyond this range, the prediction accuracy of the model will be greatly reduced. Therefore, it is of great significance to develop a more general and more suitable deviation angle model for modern high-load compressor blade profile to improve the accuracy and reliability of compressor flow design.

RESULTS AND DISCUSSION

Construction of Cascade Experiment Sample Library

In this paper, based on the High Subsonic Wind Tunnel of the National Key Laboratory, the experiment data of 24 sets of linear cascades are used as the sample library, the main geometric parameters of 24 sets of cascades and the design inlet Mach number are as shown in Table 1.

Table 1 Cascade main design parameters

cascade serial number	$\varphi(\circ)$	σ	t_b / c	a / c	f / c	e / c	Ma_d
1	40.15	2.10	0.0541	0.184	0.353	0.393	0.4
2	43.39	1.44	0.0721	0.197	0.369	0.400	0.4
3	43.38	2.356	0.0785	0.204	0.353	0.380	0.4
4	45.06	1.053	0.0939	0.236	0.372	0.387	0.4
5	51.08	2.766	0.103	0.237	0.362	0.381	0.4
6	43.22	1.723	0.115	0.276	0.383	0.393	0.4
7	49.97	1.723	0.115	0.276	0.375	0.387	0.4
8	53.77	1.723	0.115	0.262	0.359	0.374	0.4
9	14.76	1.160	0.0456	0.262	0.247	0.380	0.7
10	15.12	2.327	0.0816	0.289	0.361	0.400	0.7
11	29.12	2.327	0.0816	0.263	0.332	0.380	0.7
12	21.95	1.42	0.0972	0.289	0.382	0.400	0.7
13	36.56	1.423	0.0972	0.263	0.362	0.387	0.7
14	21.094	1.765	0.106	0.295	0.400	0.406	0.7
15	30.94	1.765	0.107	0.282	0.389	0.400	0.7
16	39.14	1.765	0.107	0.276	0.379	0.393	0.7
17	49.86	1.765	0.107	0.263	0.363	0.381	0.7
18	7.56	2.508	0.0707	0.393	0.317	0.373	0.85
19	11.78	2.508	0.0707	0.386	0.301	0.360	0.85
20	25.00	2.508	0.0707	0.406	0.276	0.341	0.85
21	25.05	1.206	0.0887	0.590	0.362	0.406	0.85
22	23.701	1.871	0.0940	0.649	0.353	0.380	0.85
23	27.56	1.871	0.0940	0.642	0.349	0.380	0.85
24	32.23	1.871	0.0940	0.642	0.336	0.367	0.85

The design parameters from left to right in the Table 1 are blade camber angle, cascade solidity, blade profile maximum relative thickness, relative position of blade profile maximum thickness, blade profile maximum relative deflection, relative position of blade profile maximum deflection and design inlet Mach number. It can be seen that the 24 sets of cascades include 8 sets of cascades with a design inlet Mach number of 0.4, 9 sets of cascades with a design inlet Mach number of 0.7, and 7 sets of cascades with a design inlet Mach number of 0.85. The Mach number range is from low subsonic to high subsonic, which can basically cover the flow condition of the cascade in the subsonic range. The geometric parameters of all the cascades also cover a large range, and the distribution is fairly homogeneous. The range of the blade camber angle ranges from a small angle of 7.56 degrees to a large stagger angle of 51.08 degrees, and the cascade solidity ranges from 1.053 to 2.766. To optimize the empirical deviation angle model, the data volume and coverage of the experimental sample library must be sufficient, so the 24 sets of linear cascades ensure the richness of geometric parameters, which is highly suitable for further correction of the subsequent empirical deviation angle model.

Error Analysis and Improvement of Deviation Angle Model

This paper selects the Lieblein reference (Lieblein S, 1957, Lieblein S, 1967) deviation angle model as the original reference deviation angle model, and its calculation formula is as follows:

$$\delta^* = (K_\delta)_{sh}(K_\delta)_t(\delta_0^*)_{10} + m\varphi \quad (1)$$

$$(\delta_0^*)_{10} = (-0.0443 + 0.1057\sigma) + (0.0209 - 0.0186\sigma)\beta_1 + (-0.0004 + 0.000\,76\sigma)\beta_1^2 \quad (2)$$

$$(K_\delta)_t = 6.25\frac{t_b}{c} + 37.5\left(\frac{t_b}{c}\right)^2 \quad (3)$$

Among them δ^* is the reference deviation angle, $(K_\delta)_{sh}$ is the correction coefficient when the blade profile is different from the NACA -65 series blade profile, and the values are shown in Table 2. The blade profile in this paper is designed independently, and it is more similar to the NACA-65 series blade profile in geometry, so the $(K_\delta)_{sh}$ is chosen as 1.0. In the subsequent process, $(K_\delta)_{sh}$ is going to be optimized as a coefficient. $(K_\delta)_t$ is the correction for the deviation angle when the blade profile thickness is not equal to the standard thickness, and it is calculated by the relative maximum thickness. $(\delta_0^*)_{10}$ is the deviation angle when the standard blade camber angle is zero, calculated by the cascade solidity σ and the inlet flow angle β_1.

Table 2 Blade profile correction factor

$(K_\delta)_{sh}$	blade profile
0.7	Double arc blade profile
1.0	NACA-65 series blade profile
1.1	C series blade profile

m is the slope of the deviation angle changing with the blade camber angle, $m_{1.0}$ is the slope when the cascade solidity is 1, and then through the function after the solidity correction, m is calculated by the following method:

$$m = \frac{m_{1.0}}{\sigma^b} \tag{4}$$

$$m_{1.0} = \begin{cases} 0.17 - 0.0333x + 0.333x^2 (NACA-65) \\ 0.249 + 0.074x - 0.132x^2 + 0.316x^3 (C-series) \end{cases}$$

$$b = 0.9625 - 0.17x - 0.85x^3 \tag{5}$$

$$x = \beta_1 / 100$$

Under the classification of inlet Mach number Ma_1, the comparison between the calculated and experimental values of the reference deviation angle is as shown in Figure 1. The closer the points in the figure are to the red line, the smaller the difference between the calculated value and the experimental value. Observe the distribution of different Ma_1 points in the entire calculation range, there are a large number of points that $Ma_1 \geq 0.7$ deviate significantly from the red line, and the calculated value is relatively small, which indicating that Ma_1 is the key to affect the calculation accuracy of the model. The smaller Ma_1 points are generally distributed around the red line, except that there is a small piece of calculation points on the right side of the figure that deviates significantly from the red line meanwhile Ma_1 is smaller. This small number of points maybe caused by the influence of other cascade parameters. To sum up, when Ma_1 is larger, it will obviously lead to inaccurate prediction of the reference deviation angle. The influence of the critical Mach number Ma_{cr} can be considered, a deviation angle correction related to the Mach number can be added when $Ma_1 \geq Ma_{cr}$, as shown in formula (6).

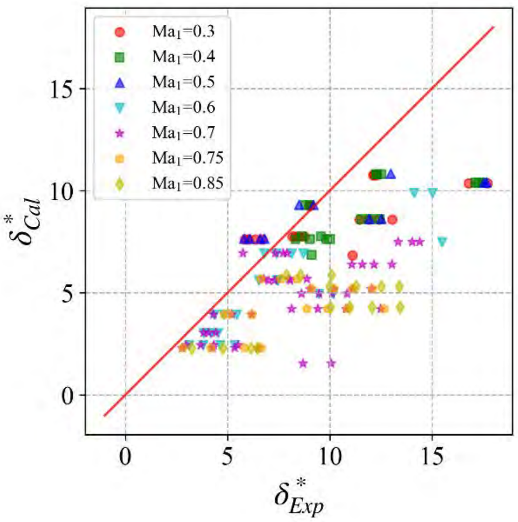

Figure 1 Predicted distribution map of deviation angle classified by inlet Mach number with reference to deviation angle model

$$\delta_{Ma}^* = \begin{cases} 0 & Ma < Ma_{cr} \\ A_1 \cdot Ma_1 \cdot (Ma_1 - Ma_{cr}) & Ma \geq Ma_{cr} \end{cases} \tag{6}$$

Because the original model doesn't show the effect of AVDR, but the establishment of the reference state is related to AVDR, different AVDR will affect the prediction of deviation angle, so the AVDR correction term such as formula (7) is added. Finally, considering that the coefficients in the original model may not be applicable to modern high-load cascades, some coefficients need a recalibration through the formula (5), such as formula (8).

$$\delta^*_{AVDR} = A_2 \cdot 10 \cdot (1 - AVDR) \tag{7}$$

$$m_{1.0} = A_3 + A_4 x + A_5 x^2$$
$$b = A_6 + A_7 x + A_8 x^3 \tag{8}$$

The Creveling model (Carmody R H and Creveling H F, 1968; Pachidis V A, 2006) is selected as the off-design deviation angle model, and its calculation formula is as follows:

$$\delta_{off} = \Delta\beta^* f(x) \tag{9}$$

$$\Delta\beta^* = \varphi + i^* - \delta^* \tag{10}$$

$$f(x) = \begin{cases} -0.809\times10^{-3} + 0.5588x - 0.2928x^2 & (x \ge 0) \\ 0.1191\times10^{-3} + 0.480x + 0.3452x^2 & (x < 0) \end{cases} \tag{11}$$

$$x = \frac{i - i^*}{\Delta\beta^*} \tag{12}$$

Where $\Delta\beta^*$ is the airflow turning angle in the reference state, and i^* is the reference incidence angle declination.

To improve the off-design deviation angle model, we must analyse the influence of different parameters on the calculation accuracy of the model first. The Mach number is undoubtedly the most important aerodynamic parameter. The calculation results of the off-design deviation angle model on different inlet Mach number conditions are shown in Figure (a). It can be seen that the distribution of the inlet Mach number is relatively uniform, so the Mach number is not the main factor affecting the error of the original model.

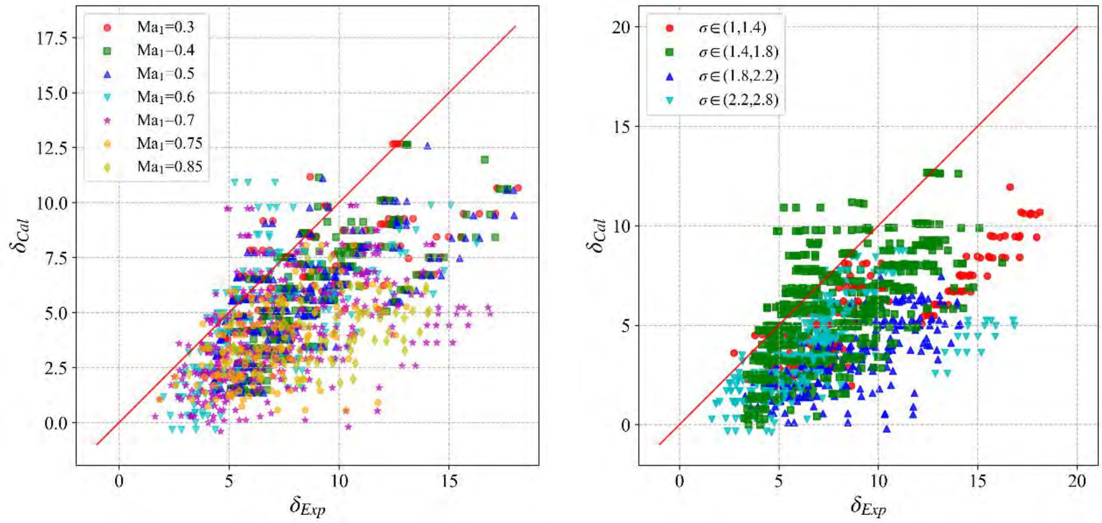

(a) Inlet Mach number distribution (b) Consistency distribution

Figure 2 Predicted distribution diagram of deviation angle of off-design deviation angle model classified by different parameters

Considering the influence of different geometric parameters on the prediction error of the model, after comparing parameters such as blade camber angle, blade profile maximum thickness, and solidity, it is found that the calculation of deviation angle is more related to the range of solidity. Figure (b) divides the solidity into four ranges, and it can be found that points in different ranges have obvious partition effects, so adding the correction term of solidity may improve the prediction accuracy of the original model.

In this paper, the form of formula (13) is used as the solidity correction coefficient of the off-design deviation angle, and the coefficient δ_{off} in the off-design deviation angle model is recalibrated, such as formula (14). The comprehensive reference deviation angle and the off-design deviation angle model are finally determined by the formula (15), where the reference deviation angle δ^* is calculated by the reference deviation angle model, and the off-design deviation angle δ_{off} is calculated by the off-design deviation angle model.

$$\delta_\sigma = \frac{1}{B_1\sigma^2 + B_2\sigma + B_3} \tag{13}$$

$$f(x) = \begin{cases} B_4 + B_5 x + B_6 x^2 & (x \ge 0) \\ B_7 + B_8 + B_9 x^2 & (x < 0) \end{cases} \tag{14}$$

$$\delta = \delta^* + \delta^*_{Ma} + \delta^*_{AVDR} + \delta_{off} \cdot \delta_\sigma \tag{15}$$

In this paper, the genetic algorithm is used to re-optimize the original coefficients and newly added coefficients in the model. First, a brief introduction to the genetic algorithm is given. Genetic algorithm (Huang M, 2019; Li H et al.,2005) is a global search optimization algorithm that simulates the natural evolution mechanism of organisms in nature. It has high robustness to different problems and powerful search capabilities and can gradually generate near optimal solution. This paper uses the traditional single-objective and single-population genetic algorithm, the coding method is real number coding, the selection algorithm uses tournament selection, the crossover algorithm is hybrid crossover method, the mutation algorithm is Gaussian mutation method, and the number of individuals in the population is 100. Note that in the process of genetic algorithm optimization coefficients, it is necessary to restrict the variation range of the coefficients, so as to avoid the original formula from losing its original physical meaning due to the excessive variation of the coefficients.

Based on the deviation angle calculation formula (15) and all the experimental points in the cascade performance experiment sample library, the root mean square error of the deviation angle as small as possible is taken as the optimization goal, and the genetic algorithm is used to optimize all coefficients. The population evolution process is shown in Figure 3, The min, max and avg in the figure represent the minimum, maximum and average values of individual fitness in the population respectively. The abscissa is the evolution algebra, and the ordinate is the root mean square error. After 200 times of evolution, the minimum and average values of individual fitness hardly change, which can be considered to have reached convergence. The 18 new coefficients obtained after optimization are shown in Table 3.

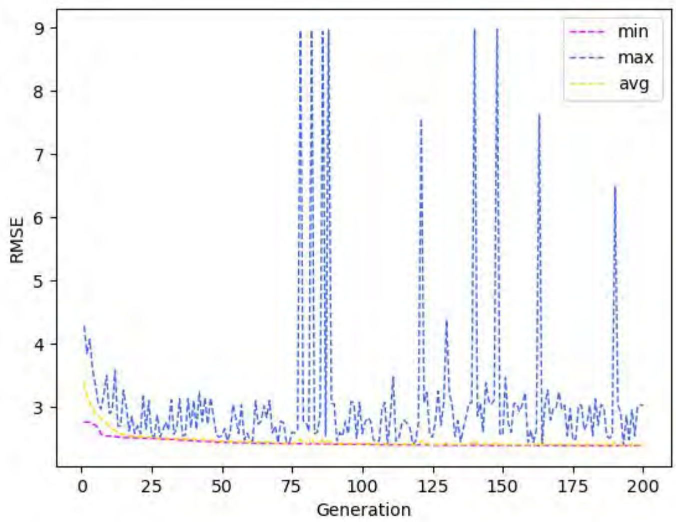

Figure 3 Genetic Algorithm Evolution Process

Table 3 Coefficient optimization results of the deviation angle improvement model

$(K_\delta)_{sh}$	A_1	A_2	A_3	A_4	A_5
0.9	29.24	0.6	0.2	-0.029	0.35
A_6	A_7	A_8	B_1	B_2	B_3
0.9603	-0.1708	-0.8213	0.001003	0.001063	1.1623
B_4	B_5	B_6	B_7	B_8	B_9
-0.0006	0.7495	-0.1003	1.910e-4	0.2805	0.3117

The deviation angle is predicted by the optimized new coefficients. Figure 4 shows the comparison of the prediction results before and after the improvement. In the figure, Ori represents the calculation result of the original model, and Aft represents the calculation result of the optimized model.

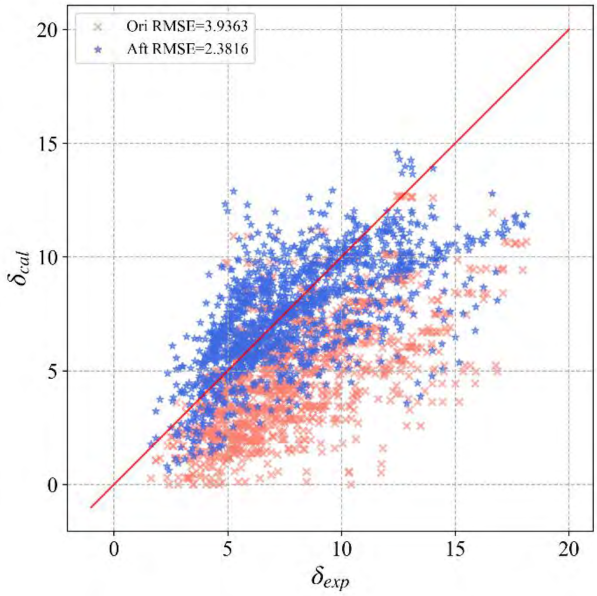

Figure 4 Comparison of the calculation results before and after the improvement of the deviation angle model

It can be seen that the calculation accuracy of the deviation angle of most points has been improved after optimization, the predicted value of the deviation angle is generally lower before the improvement. The improved calculation points are distributed near the red line, and the overall error is reduced to 60.1% of the original, which shows the effectiveness of the optimization method.

According to the improved deviation angle model, the deviation angle- incidence angle declination characteristic lines of several sets of cascades at different AVDR and inlet Mach numbers are given respectively, as shown in Fig. 5 and Fig.6.

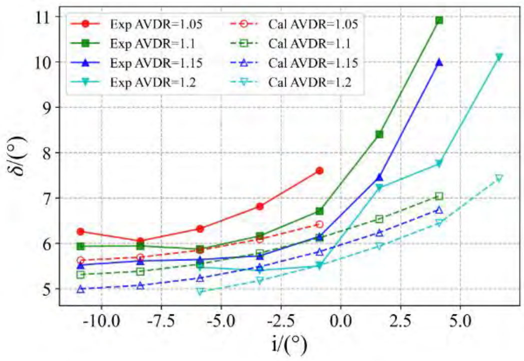

(a) Cascade No. 1 $Ma_1 = 0.4$

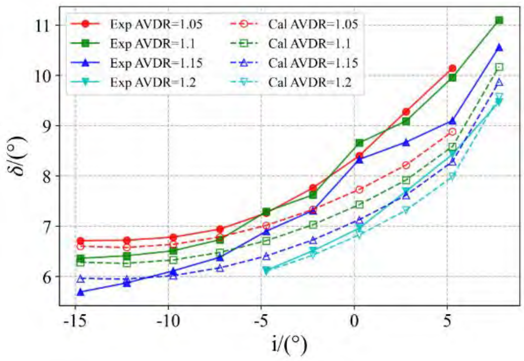

(b) Cascade No. 6 $Ma_1 = 0.4$

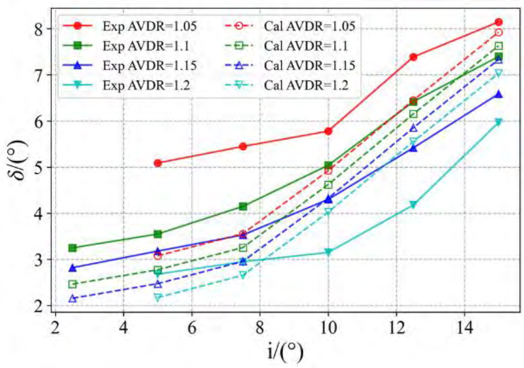

(c) Cascade No. 10 $Ma_1 = 0.7$

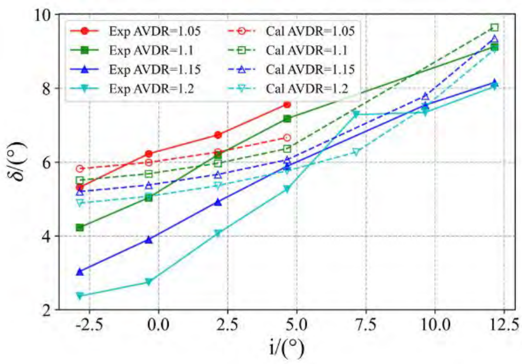

(d) Cascade No. 11 $Ma_1 = 0.7$

Fig.5 The deviation angle- incidence angle declination characteristic line of the cascade under different AVDR

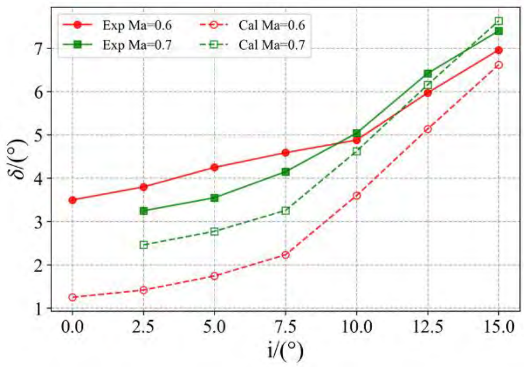

(a) Cascade No. 10 $AVDR = 1.1$

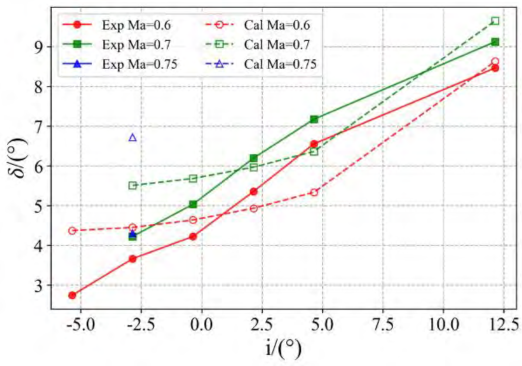

(b) Cascade No. 11 $AVDR = 1.1$

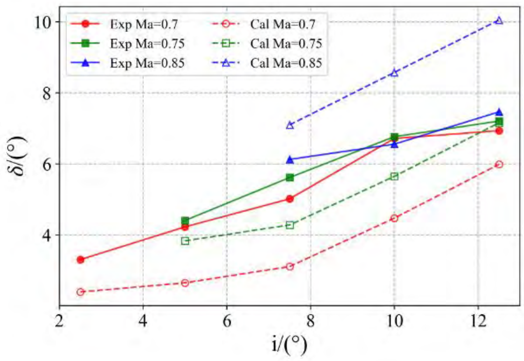

(c) Cascade No. 19 $AVDR = 1.1$

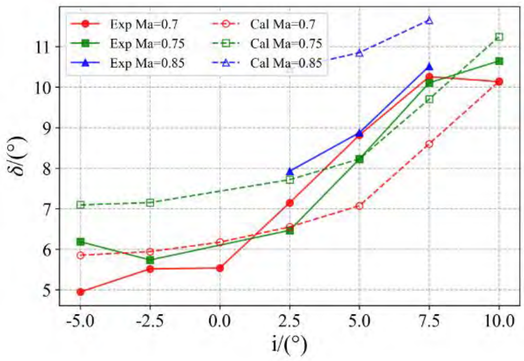

(d) Cascade No. 21 $AVDR = 1.1$

Figure 6 The deviation angle- incidence angle declination characteristic line of the cascade at different inlet Mach numbers

In Figure 5, the inlet Mach numbers of the cascades are all equal to the design Mach number. It can be seen that the deviation angle of each set of cascades has obvious changes with AVDR, and with the increase of AVDR, the deviation angle decreases, and the optimized deviation angle model also shows the same prediction effect, the local prediction value has certain errors, but the overall trend of change coincides well. In Figure 5(a), we can see that when the inlet Mach number is 0.4, the predicted value is generally lower than the experimental value under different AVDR conditions, but in Figure 5(d), when the inlet Mach number is 0.7, the predicted value is higher than the experimental value at large positive and negative incidence angle declination, and higher than the experimental value at other incidence angle declination. It can be inferred that under a large inlet Mach number, a large positive and negative incidence angle declination will lead to a high predicted value, so it can be considered to add a large incidence angle declination correction to the Mach number correction term in the subsequent work. Observing the prediction diagram drawn in Figure 6 under the working condition of AVDR = 1.1, it can be seen that even at high inlet Mach numbers, the optimized model can well follow the change of the experimental deviation angle. Under different inlet Mach numbers, the deviation angle rapid changes with increasing incidence angle declination are also predicted more accurately.

By comparing the predicted value and the experimental value of the deviation angle under different working conditions, it can be seen that the optimized deviation angle model has a smaller prediction error, and the variation trend of the experimental value is also relatively consistent, which shows the optimized model is efficient.

Calculation of Compressor Characteristics Based on Improved Empirical Model

1. Overall Characteristic Calculation

Table 4 Design parameters of multi-stage low-load compressors (Burdsall E A et al.,1979)

design variable	value
total pressure ratio	1.357
total temperature ratio	1.1008
Adiabatic efficiency	0.883
Design speed (rpm)	5455
Design flow (kg/s)	4.3

In this section, a 3.5 -stage low-load compressor with inlet guide vanes (IGV) is taken as the research object, and its design parameters are shown in Table 4. The improved deviation angle empirical model is integrated into the flow calculation program PymSCM to calculate the overall characteristic curve, and compared with the experimental results. Because the deviation angle model is corrected based on the experimental results of the subsonic linear cascade, a subsonic compressor with full working conditions is selected for calculation and verification.

The calculation results of the overall characteristics are shown in Figure 7 , in the legend Ori represents the original empirical model results, Aft represents the optimized empirical model results, and Exp represents the experimental results. In the figure, red, black and blue line represent 105 %, 100% and 85 % RPM line. It can be seen that the calculation errors of the corrected model are smaller than those of the original model at three rotational speeds, which shows that it is effective to correct the deviation angle model by using the experimental data of the linear cascade. The pressure ratio and efficiency calculated by the original model are higher, indicating that the deviation angle in the cascade channel is underestimated, while the calculated value of the improved model is closer to the real situation.

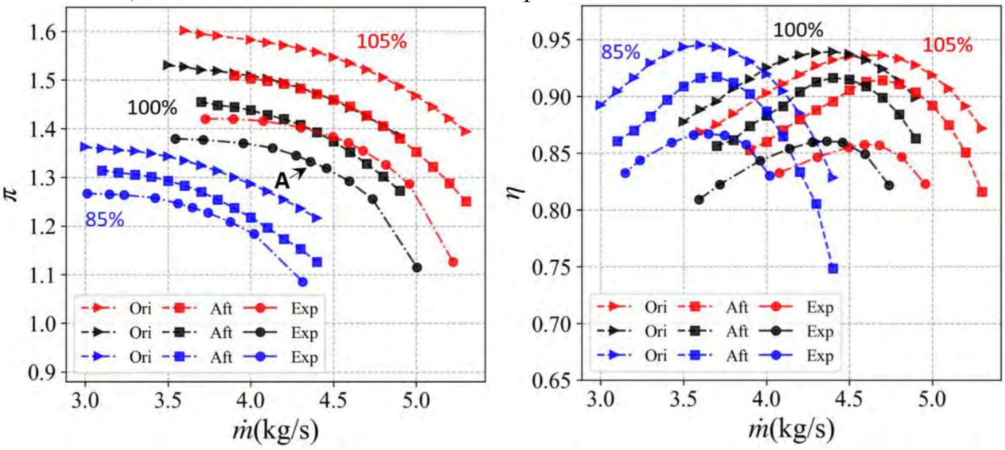

Figure 7 Calculation of Compressor Characteristics with Revised Empirical Model

Because there is no detailed interstage flow field data in the experimental report of the multi-stage compressor, it is impossible to compare the flow field calculation results with the experimental flow field calculation results, so only the design point of the design speed (point A in the figure) is selected below. The calculation results of the empirical model before and after the improvement are compared.

2. Comparison of flow field parameters

Figure 8 shows the data distribution of the deviation angle spanwise at point A calculated by the through-flow program. Because the deviation angle model used in the IGV blade row is suitable for the turbine, this paper does not improve it, so the spanwise distribution diagram of the IGV blade row is not listed, and the legend Ori in the figure indicates the calculated value of the original model, and Aft indicates the calculated value of the optimized model. From the spanwise distribution of the deviation angle, it can be seen that the deviation angle is underestimated in the original model, so the airflow turning angle in the cascade channel is higher, resulting in a higher-pressure ratio and efficiency. The improved model predicts higher deviation angles, especially at the blade tip and root, so the improved model has better predictive accuracy.

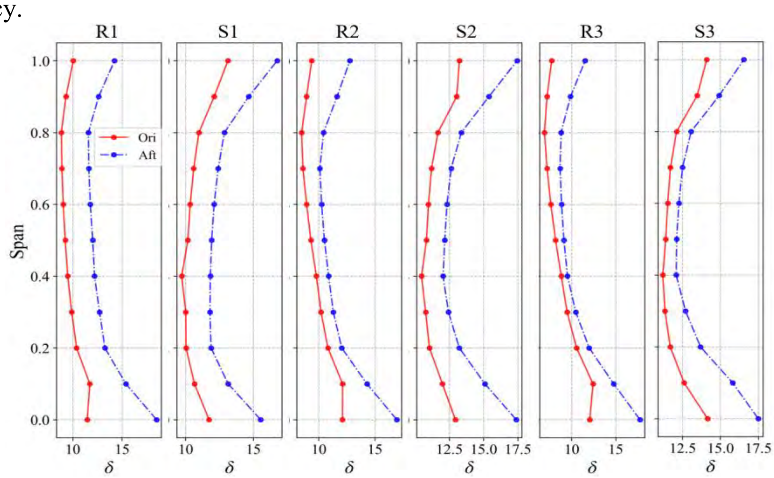

Figure 8 The spanwise distribution of deviation angle prediction values of the model before and after the improvement of working condition A

The total pressure contour obtained by the model calculation before and after the improvement of the working condition of point A is shown in Figure 9, Ori and Aft represent the calculation results of the model before and after the improvement respectively. The inlet condition of the compressor is standard atmospheric condition. With the compression of the blades row by row, the total gas pressure gradually increases. Because the predicted value of the deviation angle of the original model is low, the airflow has a larger turning angle, so the blades have made more work to the airflow. There is a significantly higher total pressure at the outlet through the cumulative effect of rows of blades, and the total pressure cloud diagram calculated by the optimized model is more consistent with the actual situation.

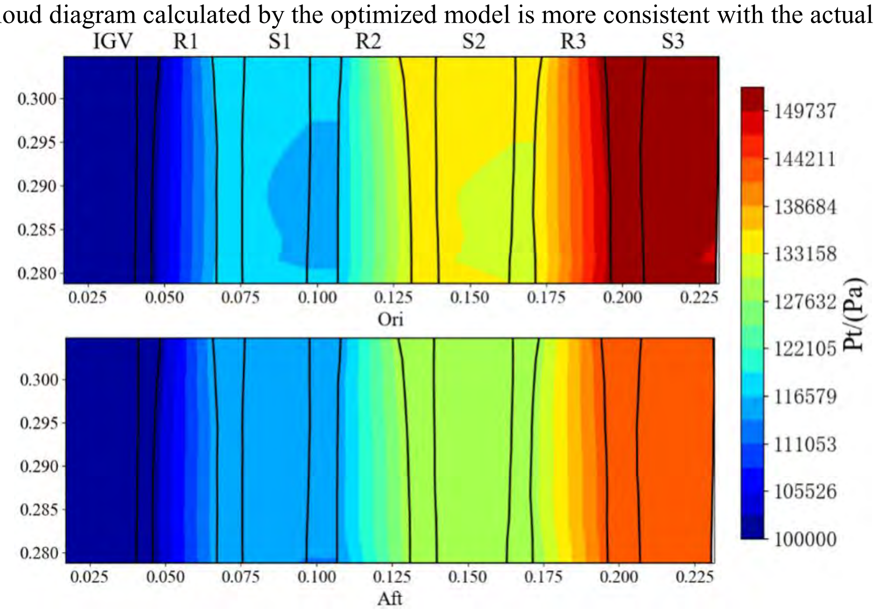

Figure 9 Comparison of the total pressure contours of the model calculation results before and after the improvement of working condition A

CONCLUSIONS

In this paper, 24 sets of linear cascades are used as geometric objects, under the consideration of diverse and reliable experimental results as much as possible, 1584 experimental operating points are finally selected as the cascade performance experiment sample library. In the second half of this paper, a typical model is selected as the original model. By analysing the error causes of the deviation angle calculation of the original model, different correction terms are added, and based on the genetic algorithm, with the experimental data as the optimization target, the deviation angle models are respectively analysed, the coefficient and the coefficient of the added term have been corrected, and the prediction error of the optimized model has been considerably improved compared with the original model. Finally, in order to further verify the new model, the characteristics of the multi-stage compressor were calculated by using the through-flow calculation program and the results were compared. It can be seen that the calculation accuracy of the revised empirical model has been greatly improved. Although the accuracy of the empirical model has been improved, there are still some differences between the predicted flow field parameters and the real flow, which reflects the difficulty of establishing an excellent deviation angle model to a certain extent.

NOMENCLATURE

φ	Blade camber angle
i	Incidence angle declination
i^*	Reference incidence angle declination
δ	Deviation angle
δ^*	Reference deviation angle
f	Blade profile maximum deflection
e	Relative position of blade profile maximum deflection
ρ	Density
γ	Blade stagger angle
Ma_1	Inlet Mach number
Ma_{cr}	Critical Mach number
Ma_d	Design inlet Mach number
β_1	Inlet airflow angle
β_2	Outlet airflow angle
σ	Cascade solidity

s	Blade spacing
c	Blade profile chord length
t_b	Blade profile maximum thickness
a	Blade profile maximum thickness position

Abbreviation

AVDR	Axial density ratio
Dev	Deviation angle
RMSE	Root mean square error
Ori	Original model
Aft	After model

ACKNOWLEDGMENTS

This work was funded by the National Major Science and Technology Projects of China (project no: 2017-II-0001-0013). The authors gratefully acknowledge the National Major Science and Technology Projects of China for their support and the permission to publish this paper.

References

Burdsall, E. A., Canal Jr, E., & Lyons, K. A. (1979). Core compressor exit stage study. 1: Aerodynamic and mechanical design (Report No. NASA-CR-160555).

Carmody, R. H., & Creveling, H. F. (1968). Axial flow compressor computer program for calculating off-design performance (Program 4) (Report No. NASA CR-121770).

Huang, M. (2019). Optimization design of compressor forward problem based on neural networks and genetic algorithm (Doctoral dissertation). Nanjing University of Aeronautics and Astronautics.

Lieblein, S. (1957). Analysis of experimental low-speed loss and stall characteristics of two-dimensional compressor blade cascades (Report No. NACA-TN-3923).

Lieblein, S. (1960). Incidence and deviation-angle correlations for compressor cascades. Journal of basic Engineering, pp. 195-203.

Li, H., Xie, S., & Yi, Z. (2005). Principles and applications of genetic algorithm. Mining and Metallurgy, (01), pp. 87-90.

Novak, R. A. (1967). Streamline curvature computing procedures for fluid-flow problems. Journal of Engineering for Power, pp. 478-490.

Pachidis, V. A. (2006). Gas Turbine Advanced Performance Simulation (Doctoral dissertation). Cranfield University.

Wu, X., Liu, B., & Tang, T. (2017). Application of streamline curvature method in predicting characteristics of multi-stage transonic axial compressors. Propulsion Technology, (10), pp. 2235-2245.

Wu, C. (1952). A general theory of three-dimensional flow in subsonic and supersonic turbomachines of axial-, radial, and mixed-flow types (Report No. NASA-TM-1024). Washington, DC: National Aeronautics and Space Administration.

Xu, J. (2017). Mr. Wu Zhonghua and the theory of three-dimensional flow in turbomachinery. Propulsion Technology, 38(10), pp. 2161-2163.